Rotation sequence to report humerothoracic kinematics during 3D motion involving large horizontal component: application to the tennis forehand drive

Thomas Creveaux, Violaine Sevrez, Raphaël Dumas, Laurence Cheze, Isabelle Rogowski

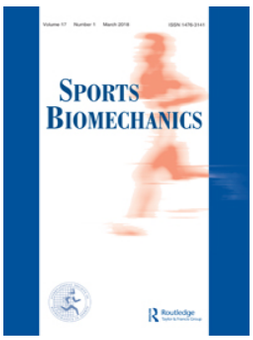

Sports Biomechanics

ISSN: 1476-3141 (Print) 1752-6116 (Online) Journal homepage: http://www.tandfonline.com/loi/rspb20

Rotation sequence to report humerothoracic kinematics during 3D motion involving large horizontal component: application to the tennis forehand drive

Thomas Creveaux, Violaine Sevrez, Raphaël Dumas, Laurence Chèze & Isabelle Rogowski

To cite this article: Thomas Creveaux, Violaine Sevrez, Raphaël Dumas, Laurence Chèze & Isabelle Rogowski (2018) Rotation sequence to report humerothoracic kinematics during 3D motion involving large horizontal component: application to the tennis forehand drive, Sports Biomechanics, 17:1, 131-141, DOI: 10.1080/14763141.2016.1260765

To link to this article: https://doi.org/10.1080/14763141.2016.1260765

Published online: 28 Feb 2017.

Routledge
Taylor & Francis Group

Sports Biomechanics, 2015

Vol. X, No. X, 1–3, http://dx.doi.org/xxxxxxxxxxxxx

Word count (Introduction through Conclusion): 3150

ORIGINAL RESEARCH

ROTATION SEQUENCE TO REPORT HUMEROTHORACIC KINEMATICS DURING 3D MOTION INVOLVING LARGE HORIZONTAL COMPONENT: APPLICATION TO THE TENNIS FOREHAND DRIVE

Thomas Creveaux[1,2], Violaine Sevrez[1,2], Raphaël Dumas[1,3], Laurence Chèze[1,3], & Isabelle Rogowski[1,2]

[1] *Université de Lyon, Lyon, France; Université Lyon 1, Lyon, France*

[2] *Centre de Recherche et d'Innovation sur le Sport - EA 647; UFRSTAPS; 27-29, boulevard du 11 novembre 1918, 69622 Villeurbanne Cedex, France*

[3] *IFSTTAR, UMR_T9406, LBMC Laboratoire de Biomécanique et Mécanique des Chocs, F69675, Bron*

Thomas Creveaux, Centre de Recherche et d'Innovation sur le Sport - EA 647; UFRSTAPS; 27-29, boulevard du 11 novembre 1918, 69622 Villeurbanne Cedex, France, + 33 4 72 43 28 48, thomas.creveaux@univ-lyon1.fr

Rotation sequence to report humerothoracic kinematics during 3D motion involving large horizontal component: application to the tennis forehand drive

Violaine Sevrez, Centre de Recherche et d'Innovation sur le Sport - EA 647; UFRSTAPS; 27-29, boulevard du 11 novembre 1918, 69622 Villeurbanne Cedex, France, + 33 4 72 43 28 48, violaine.sevrez@univ-lyon1.fr

Raphaël Dumas, Laboratoire de Biomécanique et Mécanique des Chocs – UMR_T 9406 - IFSTTAR; 43, boulevard du 11 novembre 1918, 69622 Villeurbanne Cedex, France, +33 4 72 44 85 75, raphael.dumas@ifsttar.fr

Laurence Chèze, Laboratoire de Biomécanique et Mécanique des Chocs – UMR_T 9406 - IFSTTAR; 43, boulevard du 11 novembre 1918, 69622 Villeurbanne Cedex, France, +33 4 72 44 80 98, laurence.cheze@univ-lyon1.fr

---

Corresponding author:

Isabelle ROGOWSKI

UCB Lyon 1 – UFRSTAPS – CRIS EA 647

27-29, bd du 11 novembre 1918 - 69622 Villeurbanne Cedex, France

Tel: + 33 4 72 43 28 48; Fax: + 33 4 72 44 80 10

E-mail: isabelle.rogowski@univ-lyon1.fr

Funding acknowledgement

This study was supported by the "Agence Nationale pour la Recherche" and the "pôle de Compétitivité Sporaltec" [ANR ACE n°2010-BLANC-901].

Conflict of interest statement

The authors declare that there is no conflict of interest.

Abstract

The aim of this study was to examine the respective aptitudes of three rotation sequences ($Y_tX_f'Y_h$", $Z_tX_f'Y_h$" and $X_tZ_f'Y_h$") to effectively describe the orientation of the humerus relative to the thorax during a movement involving a large horizontal abduction / adduction component: the tennis forehand drive. An optoelectronic system was used to record the movements of eight elite male players performing ten forehand drives. The occurrences of gimbal lock, phase angle discontinuity and incoherency in the time course of the three angles defining humerothoracic rotation were examined for each rotation sequence. Our results demonstrated that no single sequence effectively describes humerothoracic motion without discontinuities throughout the forehand motion. The humerothoracic joint angles can nevertheless be described without singularities when considering the backswing/forward-swing and the follow-through phases separately. Our findings stress that the sequence choice may have implications for the report and interpretation of 3D joint kinematics during large shoulder range of motion. Consequently, the use of Euler/Cardan angles to represent 3D orientation of humerothoracic joint in sport tasks requires the evaluation of the rotation sequence regarding singularity occurrence before analysing the kinematic data, especially when the studied motion involves a large range of motion at the shoulder.

Abstract word count: 195

Key-words: Phase angle discontinuity, Euler/Cardan convention; gimbal-lock; joint angle coherence; shoulder

Rotation sequence to report humerothoracic kinematics during 3D motion involving large horizontal component: application to the tennis forehand drive

Introduction

Limb orientation has been extensively used to characterise important features of human movement such as performance (Harrison, Ryan, & Hayes, 2007) or variability (Sides & Wilson, 2012). Movement analysis thus requires reliable descriptions of segment orientations, which can be either based on individual limb orientations by mean of projection angles (Elliott, Takahashi, & Noffal, 1997; Owens & Lee, 1969; Whiteside, Elliott, Lay, & Reid, 2013) or relative limb orientations by mean of helical (screw) axes (Baeyens, Van Roy, De Schepper, Declercq, & Clarijs, 2001; Phadke, Braman, LaPrade, & Ludewig, 2011; Sahara, Sugamoto, Murai, Tanaka, & Yoshikawa, 2006 ; Woltring, Huiskes, De Lange, & Veldpaus,1985; Kelkar et al., 2001), dual Euler angles (Teu, Kim, Fuss, & Tan, 2006; Ying & Kim, 2002) or Euler / Cardan angles (Karduna, McClure, & Michener, 2000 ; Phadke et al., 2011). Euler / Cardan angle rotation sequences have been recommended (Wu et al., 2002, Wu et al., 2005), unlike Helical axis systems, because they can be used as a physiologically meaningful framework for investigating both kinematics and kinetics.

Twelve Euler/Cardan rotation sequences exist, based on the ordering of three rotations about an axis of the proximal segment, a floating axis and an axis of the distal segment. Care must thus be taken when choosing a particular rotation sequence, as matrix multiplication is not commutative and several studies have documented significant differences in angular kinematics between various angle conventions and sequences (Senk & Chèze, 2006; Karduna et al., 2010; Sinclair et al., 2012; Bonnefoy-Mazure et al., 2010; Phadke et al., 2011). Indeed, each of the three-rotation permutations differently defines the magnitudes of the three rotation angles, possibly leading to incoherent joint amplitude. The decomposition into Euler/Cardan angles may further lead to two other types of singularities in time histories of the angle values (van der Helm, 1997). First, when approaching the so-called “gimbal lock” position (i.e., when the first

and third rotation axes coincide), the computed angle values become very sensitive to joint motion, resulting in physiologically meaningless angle variations. Second, the necessary use of inverse trigonometric functions can result in phase angle discontinuities, characterised by large absolute differences, up to 360°, between two successive angle values.

The shoulder complex has the greatest range of motion compared to other body joints, due to the synchronised movement of three bones and five joints. To overcome such complexity, the shoulder is frequently modelled as a unique virtual "humerothoracic joint" by ignoring the scapula and clavicle bones. Since this simplification is conducive to larger ranges of motion when describing shoulder joint mechanics, these rotations also become more susceptible to gimbal lock. In order to address issues related to the selection of a particular sequence, the International Society of Biomechanics (ISB) has established standards for reporting kinematics and recommended specific rotation sequences in order to describe the 3D orientation of given human joints so that the angles remain as close as possible to the clinical definitions of joint and segment motions (Wu et al., 2002, Wu et al., 2005). For the motion of the humerus relative to the thorax, the $Y_tX_f'Y_h"$ sequence has been proposed (Wu et al., 2005), corresponding to the first Y_t axis belonging to the thorax, the last $Y_h"$ axis belonging to the humerus and the intermediate X_f' axis being a floating axis. However, previous studies have shown that, even when considering the glenohumeral joint, which is likely to result in smaller ranges of motion compared to those obtained from humerothoracic one, no single rotation sequence satisfies the criteria to describe all motions across all available ranges without singularity (Senk & Chèze, 2006). Moreover, research has traditionally examined planar movements when developing recommendations for using different rotation sequences (Phadke et al., 2011; Senk & Chèze, 2006), so it remains unclear if these are appropriate for describing complex sporting motions such as tennis strokes.

Rotation sequence to report humerothoracic kinematics during 3D motion involving large horizontal component: application to the tennis forehand drive

Reliable descriptions of humerothoracic joint motion are crucial to understanding the role of the shoulder joint in performance and injury until more reliable methods to document scapula-humeral motion are developed. Previously, the use of $Y_tX_f'Y_h$" sequence to estimate humerothoracic angles during the tennis flat serve has been shown to result in gimbal locks (Bonnefoy-Mazure et al., 2010), which are likely to occur as the humerus longitudinal axis Y_h and thorax vertical axis Y_t become more closely aligned. According to this study, $X_tZ_f'Y_h$" should be the preferred sequence for describing shoulder joint rotations during the serve. Although the tennis forehand drive involves large horizontal abduction / adduction range of motion, the validity of the rotation sequence recommended by the ISB to describe the humerothoracic joint angles has not yet been demonstrated. Especially, the issues related to potential occurrences of singularities have not been investigated. As a consequence, the $Y_tX_f'Y_h$" rotation sequence, as well as other rotation sequences, should be evaluated in order to describe large horizontal abduction / adduction motions at the shoulder joint without mathematical singularities and, in turn, propose an appropriate humerothoracic 3D angle interpretation.

The purpose of the present study was to determine which rotation sequence, if any, could be used to obtain singularity-free humerothoracic joint kinematics during the tennis forehand drive, a stroke involving a large horizontal abduction/adduction range of motion of the humerus relative to the thorax. It was hypothesised that such description of the humerothoracic joint motion during the tennis forehand drive cannot be achieved when using a single rotation sequence but rather may be accomplished by using distinct rotation sequences before and after ball-racket impact.

Methods

On an inside hard tennis court, eight competitive male tennis players (age = 26.7 ± 4.4 years, height = 1.79 ± 0.04 m, mass = 76.3 ± 6.0 kg, International Tennis Number: 3) hit 10 balls projected by a ball machine using flat forehand drive. This study was approved by the ethical committee "Sud-Est II", and informed consent was obtained directly from each participant.

Eight passive reflective markers (16 mm diameter) were glued over the following bony landmarks: incisura jugularis, xiphoid process, C7, T8, and, on the dominant side, angulus acromialis, deltoïdus tuberosity, medial and lateral epicondyles of the elbow (Creveaux et al., 2013). An additional marker was placed at the top of the racket handle, and the ball was covered with reflective adhesive tape. An eight digital-camera opto-electronic Motion Analysis system (500 Hz, Santa Rosa, California) was used to record the 3D trajectories of the markers during play. This study considered the classical simplification of the entire shoulder complex by analysing only the rotations of the humerus Segment Coordinate System (SCS) (X_h, Y_h, Z_h) relative to the thorax SCS (X_t, Y_t, Z_t) as represented in Figure 1. Raw marker coordinates where smoothed according to the procedure defined by Creveaux et al. (2013) and used to build the SCS for each body segment according to the ISB recommendations (Wu et al., 2005). The humerothoracic joint centre was determined by regression (Dumas, Chèze & Verriest, 2007) in a static posture.

Insert Figure 1 near here

Three rotation sequences were tested: the $Y_tX_f'Y_h$" Euler sequence recommended for the shoulder by the ISB (Wu et al., 2005), and the $Z_tX_f'Y_h$" and $X_tZ_f'Y_h$" Cardan sequences respectively recommended for most joints by the ISB (Wu et al., 2002, Wu et al., 2005) and

demonstrated as efficient for glenohumeral joint during analytical motions (Senk & Chèze, 2006) and for humerothoracic joint during the tennis serve (Bonnefoy-Mazure et al., 2010).

For the subsequent analysis, the forehand drive was both considered as a whole, and as the succession of three independent phases: the backswing, the forward swing and the follow-through (Ryu, McCormick, Jobe, Moynes, & Antonelli, 1988). The backswing was defined from the first to the last frames of racket backward motion. The forward swing ended two frames before impact. The follow-through began two frames after impact and lasted until the elbow reached its maximal height. Frames surrounding the impact were removed in order to prevent issues associated with data smoothing through the impact (Knudson & Bahamonde, 2001). Using such definitions, stroke phases were defined independently of humerothoracic angles.

The time course of the three angles defining humerothoracic rotation were computed for each of the three rotation sequences, and analysed to assess for occurrence of the three singular cases, (gimbal locks, phase angle discontinuities, and amplitude incoherencies) both throughout the forehand drive and for each of the three phases of the stroke considered independently. Gimbal locks were assumed to occur when the absolute difference between the second rotation angle at a given time and the gimbal lock value ($k\pi$ for $Y_tX_f'Y_h$", $\pi/2+k\pi$ for $X_tZ_f'Y_h$" and $Z_tX_f'Y_h$", where k is any integer) ranged from 0 to 20° for Euler angles, and from 0 to 10° for Cardan angles (Senk & Chèze, 2006). For each of the three angles of each of the three rotation sequences, occurrence of gimbal locks was quantified as the number of subjects for which at least one gimbal lock was observed among the 10 analysed trials and as the percentage of frames for which gimbal locks were detected. Phase angle discontinuities were considered to occur when the absolute angular difference between two consecutive frames was higher or equal to 180°. For each of the three angles of each of the three rotation sequences, the first (*F*) and last

(*L*) extrema (i.e., maximum or minimum) were extracted from the experimental data. The corresponding amplitude was then defined as *L-F*. The amplitude coherences were first evaluated from the amplitude standard deviations, as large values are likely to be related to inconsistent joint histories across subjects and trials. Furthermore, the mean amplitudes were compared with the range of shoulder motion previously reported in the literature (Kapandji, 1980; Sarrafian, 1992) in order to identify angle histories which are likely to be described by excessive amplitudes regarding human anatomical range of motion.

Finally, as $X_tZ_f'Y_h$" and $Z_tX_f'Y_h$" describe the humerothoracic joint with angles that can be interpreted the same (flexion / extension, elevation and axial rotation angles are used to describe both rotation sequences while $Y_tX_f'Y_h$" one relies on the plane of elevation orientation), the absolute differences between the joint angles were measured at ball-racket impact (where the axes of both sequences are assumed rather coincident). These differences were used to quantify the discontinuity resulting from using one of these sequences before ball-racket impact and the other after it.

For each of the aforementioned parameters, the mean and standard deviations values presented in the tables were computed from the average of the 10 individual trials.

Results

Insert Table 1 near here

Insert Figure 2 near here

Gimbal lock

Rotation sequence to report humerothoracic kinematics during 3D motion involving large horizontal component: application to the tennis forehand drive

Considering the whole movement, gimbal lock occurred for all of the studied rotation sequences (Table 1). This was however not the case when considering the three phases of the stroke separately (Figure 2). During the backswing of the forehand drive, gimbal locks were observed for $Y_tX_f'Y_h$" and $Z_tX_f'Y_h$" sequences, but not for $X_tZ_f'Y_h$". For the forward swing phase, they occurred for $Y_tX_f'Y_h$" and $Z_tX_f'Y_h$" sequences, but not for $X_tZ_f'Y_h$". Regarding the follow-through phase, gimbal locks occurred for $X_tZ_f'Y_h$" sequence only.

Phase angle discontinuity

Insert Table 2 near here

Considering the whole movement, phase angle discontinuities appeared in each of the three rotation sequences (Table 2). A separate investigation of the three phases revealed that phase angle discontinuities occurred in all phases when using $Y_tX_f'Y_h$" sequence (Figure 2a), in the back- and forward swing for $Z_tX_f'Y_h$" sequence (Figure 2b), and only during the follow-through phase for $X_tZ_f'Y_h$" sequence (Figure 2c).

At ball-racket impact, the absolute differences between the angles obtained from $X_tZ_f'Y_h$" and $Z_tX_f'Y_h$" rotation sequences were 5.0 ± 2.3 °, 6.2 ± 3.3 ° and 19.1 ± 5.0 ° for flexion / extension, elevation and axial rotation, respectively (Figure 2d).

Amplitude coherence

Considering the whole stroke, the standard deviations of the humerothoracic angular amplitudes reported for the first and third angles displayed high values compared to the amplitude means whatever the chosen rotation sequence (Table 3). To a lesser extent, this was also observed in all forehand drive phases when using $Y_tX_f'Y_h$" sequence, as well as during the forward swing and follow-through phases for the $Z_tX_f'Y_h$" and $X_tZ_f'Y_h$" sequences, respectively.

Insert Table 3 near here

Discussion and Implications

The present study showed that singularities affected each of the joint angle time histories obtained when using three rotation sequences (Y_tX_f'Y_h", Z_tX_f'Y_h" and X_tZ_f'Y_h") to describe the orientation of the humerus relative to the thorax during a movement involving an expansive horizontal abduction/adduction: the forehand drive in tennis.

This study brings new knowledge regarding singularity occurrence in joint angle time histories. Indeed, while previous works reported the occurrence of gimbal locks and phase angle discontinuities as a number of trials or subjects only (Bonnefoy-Mazure et al., 2010; Senk & Chèze, 2006), the present work is the first to also quantify the proportion of frames affected by the gimbal locks. Although gimbal locks did not affect every subject and, where present, only occurred in a small percentage of frames (Table 1), this would still introduce considerable error to the measured joint rotations (Table 3; Figure 2b and 2c) and the corresponding descriptive statistics (e.g., mean, standard deviation, extrema). Especially, gimbal locks resulted in abnormally important and abrupt evolution of joint angles (Figure 2b and 2c), hence preventing the humerothoracic angle time courses from being appropriately quantified. The singularities due to gimbal lock cannot be post-processed, as opposed to phase angle discontinuities. Nevertheless, the phase angle discontinuities were not corrected in the present study in order to quantify their occurrence. As a consequence, the incoherencies in angle amplitude are mainly due to these discontinuities as well as to the singularities. On the contrary, the coherences in angle amplitude reveal that the rotation sequence is not only free of singularities and discontinuities but additionally reveal that the joint angle allow for a physiological interpretation.

Rotation sequence to report humerothoracic kinematics during 3D motion involving large horizontal component: application to the tennis forehand drive

The main finding of this study is that no single rotation sequence satisfied the three criterions to effectively describe humerothoracic motions throughout the forehand drive, thus confirming that care should be taken to avoid misinterpretation of kinematic data (Bonnefoy-Mazure et al., 2010, Phadke et al., 2011). Indeed, gimbal locks and/or phase angle discontinuities (Tables 1 and 2, Figure 2) causing joint angle incoherencies (Table 3) were observed for all three rotation sequences at some part of the movement.

From the literature, the maximal anatomical amplitude of the shoulder rotation angles has been reported to attain to 210 degrees for plane of elevation orientation and flexion/extension, 190 degrees for axial rotation and 230 degrees for elevation (Kapandji, 1980). The range of motion observed in this work when using $X_tZ_f'Y_h$" before impact and $Z_tX_f'Y_h$" after impact did not exceed these limits of human shoulder anatomical amplitudes (Table 3) and was also compatible with the functional characteristics of the upper limb described more recently (Sarrafian, 1992). Conversely, exaggerated variability of joint angles amplitude was observed when using $Z_tX_f'Y_h$" before impact and $X_tZ_f'Y_h$" after impact, so that these sequences should not be used to describe the humerothoracic angles during the corresponding forehand drive phases. Such extreme variability was also observed when using $Y_tX_f'Y_h$" rotation sequence whatever the considered motion phase, hence preventing reliable description of the motion.

A more thorough examination of the results nevertheless revealed that humerothoracic joint angles could be described coherently and without singularities only if the stroke was divided into parts. Admittedly, the $Y_tX_f'Y_h$" and $Z_tX_f'Y_h$" sequences unavoidably generate gimbal locks before impact since they occur as soon as humerus elevation angle approaches 0 (Figure 2a) or 90° (Figure 2b) respectively. But the $X_tZ_f'Y_h$" sequence should be effective in describing the "before impact" part of the stroke as neither singularity nor incoherency were

reported during the backswing and forward swing phases (Figure 2c). This observation is in agreement with previous results which demonstrated this sequence to be effective for describing the elevation of the humerus in the scapular or frontal planes (Senk & Cheze, 2006).

Similar observations were driven for the "after impact" part of the stroke. Indeed neither the $Y_tX_f'Y_h$" (Figure 2a) nor the $X_tZ_f'Y_h$" (Figure 2c) sequences were effective in reporting humerus orientation during the follow-through, but the $Z_tX_f'Y_h$" (Figure 2b) sequence was. In accordance with earlier experiments (Senk & Cheze, 2006), the $X_tZ_f'Y_h$" sequence produced gimbal locks due to the arm crossing the midline of the body in the direction of horizontal adduction. As previously reported for analytical movements (Phadke et al., 2011), phase angle discontinuities occurred in the time history of the angle related to the rotation around the humerus longitudinal axis for the $Y_tX_f'Y_h$" sequence, with abrupt changes from internal to external rotated positions. Thus, only the $Z_tX_f'Y_h$" sequence appears to effectively describe post-impact shoulder joint kinematics as neither singularity nor incoherency were reported during the follow-through phase of the stroke.

Taken together, the results of this work showed that none of the studied rotation sequences sufficiently well described the humerothoracic kinematics during the whole stroke, but that different rotation sequences may be applied to the different phases of the forehand drive. However, it should be noted that, while the use of several rotation sequences allows for a reliable description of the 3D angles for different sections of the movement, it may induce further discontinuities of joint angles at section endpoints. As opposed to phase angle discontinuities (at least 180°) and large ranges of motion arising from gimbal locks, the discontinuities due to the combination of sequences are expected of relative low amplitude. In this study, the absolute differences between the angles obtained at ball-racket impact from $X_tZ_f'Y_h$" and $Z_tX_f'Y_h$" rotation sequences may be considered to reflect important discrepancies in the description of the rotation angles, especially for the axial rotation (Figure 2d). However,

these differences were lower than the calculation errors observed near the singularities when using a single rotation sequence throughout the whole motion (Figure 2). From a general point of view, switching from a rotation sequence to another should be done in a manner that favours consistency in the description of joint angles throughout the different phases. In other words, instants for which the angles obtained from the chosen sequences are closest from each other should be looked for and considered as first choices for switching between the rotation sequences. In this perspective, providing a physiologically meaningful motion splitting to make sense from a technical point of view should also be a concern. We also recommend that when the motion is split in several phases and described with different rotation sequences, the discontinuity in the angle time history at the phases' endpoints should be quantified as well as the angular range of motion during these phases. Moreover, in order to provide the most complete information, the joint angles obtained at the split instants should be reported for both rotation sequences used before and after it.

Some limitations can be considered regarding the present study, without however questioning the results obtained from this work. First, as the joint angles were computed from the data acquired from an optoelectronic system, the measurements suffer from classical issues of motion analysis such as "soft tissue artefacts". Furthermore, until now, the time course of humerothoracic joint angles during the forehand drive has not been described using singularity-free rotation sequences, so that the results of this study could not be compared to gold standard data. More generally, as this is the case for all three-dimensional studies, it is difficult to know the extent to which the obtained kinematics are valid. Finally, the present results may not be generalized to specific tennis player populations regarding age, gender or skill level, as the motion kinematics can differ according to these characteristics.

Conclusion

In conclusion, our findings may have two primary implications for the interpretation and reporting of 3D humerothoracic joint kinematics. Firstly, these data confirm that no Euler / Cardan angle rotation sequence (non-Helical axis system) can clearly define joint rotations without discontinuities. Therefore, the methodology proposed in this paper (i.e. testing different rotation sequences, verifying occurrence of gimbal lock, phase angle discontinuity and amplitude coherence) should precede future reporting of specific humerothoracic movements to ensure that the measured humerothoracic joint kinematics are most likely to be accurate. Secondly, in cases where the gimbal-lock problem cannot be resolved using a single rotation sequence, as it often is the case when large abduction range of motion are observed (Rab, Petuskey, & Bagley, 2002) such as in throwing motions, the movement should be divided into parts, defined adequately to make sense from the coaches and sportsmen perspective and to favour the consistency in the description of the joint angle time history from different rotation sequences. Last but not least, information regarding the rotation sequence(s) used in the analysis should be detailed in any paper for the sake of clarity, reproducibility, and potential comparison, as different rotation sequences are likely to lead to different results.

Funding acknowledgement

This study was supported by the "Agence Nationale pour la Recherche" and the "Pôle de Compétitivité Sporaltec" [ANR ACE n°2010-BLANC-901].

Conflict of interest statement

The authors declare that there is no conflict of interest.

References

Baeyens, J.P., Van Roy, P., De Schepper, A., Declercq, G., & Clarijs, J.P. (2001). Glenohumeral joint kinematics related to minor anterior instability of the shoulder at the end of the late preparatory phase of throwing. *Clinical Biomechanics*, 16, 752-757. doi: 10.1016/S0268-0033(01)00068-7

Bonnefoy-Mazure, A., Slawinski, J., Riquet, A., Lévèque, J.-M, Miller, C., & Chèze, L. (2010). Rotation sequence is an important factor in shoulder kinematics. Application to the elite players' flat serves. *Journal of Biomechanics*, 43, 2022-2025. doi: 10.1016/j.jbiomech.2010.03.028

Creveaux, T., Dumas, R., Hautier, C., Macé, P., Chèze, L., & Rogowski, I. (2013). Joint kinetics to assess the influence of the racket on a tennis player's shoulder. *Journal of Sports Science and Medicine*, 12. Retrieved from: http://www.jssm.org/vol12/n2/6/v12n2-6text.php

Dumas, R., Cheze, L., & Verriest, J.-P (2007). Adjustments to McConville et al. and Young et al. body segment inertial parameters. *Journal of Biomechanics*, 40, 543-553. doi: 10.1016/j.jbiomech.2006.02.013

Elliott, B., Takahashi, K., & Noffal, G. (1997). The Influence of Grip Position on Upper Limb Contributions to Racket Head Velocity in a Tennis Forehand. *Journal of Applied Biomechanics*, 13, 182. Retrieved from http://journals.humankinetics.com/jab-back-issues

Harrison, A.J., Ryan, W., & Hayes, K. (2007). Functional data analysis of joint coordination in the development of vertical jump performance. *Sports Biomechanics*, 6, 199-214. doi: 10.1080/14763140701323042

Kapandji, I.A. (1980). The Physiology of the Joints: Upper Limb, Volume 1 (5th ed.). Churchill Livingstone.

Karduna, A.R., McClure, P.W., & Michener, L.A. (2000). Scapular kinematics: effects of altering the Euler angle sequence of rotations. *Journal of Biomechanics*, 33, 1063-8. doi: 10.1016/S0021-9290(00)00078-6

Kelkar, R., Wang, V.M., Flatow, E.L., Newton, P.M., Ateshian, G.A., Bigliani, L.U., … Mow V.C. (2001). Glenohumeral mechanics: a study of articular geometry, contact, and kinematics. *Journal of Shoulder and Elbow Surgery*, 10, 73-84. doi: 10.1067/mse.2001.111959

Knudson, D., & Bahamonde, R. (2001). Effect of endpoint conditions on position and velocity near impact in tennis. *Journal of Sports Sciences*, 19, 839-44. doi: 10.1080/026404101753113787

Owens, M.S., & Lee, H.Y. (1969). A determination of velocities and angles of projection for the tennis serve. *Research Quarterly. American Association for Health, Physical Education and Recreation*, 40, 750-754. doi: 10.1080/10671188.1969.10614914

Phadke, V., Braman, J.P., LaPrade, R.F., & Ludewig, P.M. (2011). Comparison of glenohumeral motion using different rotation sequences. *Journal of Biomechanics*, 44, 700-705. doi: 10.1016/j.jbiomech.2010.10.042

Rab, G., Petuskey, K., & Bagley, A. (2002). A method for determination of upper extremity kinematics. *Gait & Posture*, 15, 113-119. doi: 10.1016/S0966-6362(01)00155-2

Ryu, R., McCormick, J., Jobe, F., Moynes, D., & Antonelli, D. (1988). An electromyographic analysis of shoulder function in tennis player. *American Journal of Sports Medicine*, 16, 481-485. doi: 10.1177/036354658801600509

Sahara, W., Sugamoto, K., Murai, M., Tanaka, H., & Yoshikawa, H. (2006). 3D kinematic analysis of the acromioclavicular joint during arm abduction using vertically open MRI. *Journal of Orthopaedic Research*, 24, 1823-31. doi: 10.1002/jor.20208

Sarrafian, S.K. (1992), Kinesiology and Functional Characteristics of the Upper Limb. In Bowker, J.H., & Michael, J.W. (Eds), Atlas of Limb Prosthetics: Surgical, Prosthetic, and

Rehabilitation Principles (2nd edition, pp. 83-106). Rosemont, IL, American Academy of Orthopedic Surgeons. Available from http://www.oandplibrary.org/alp/chap05-01.asp

Senk, M., & Chèze, L. (2006). Rotation sequence as an important factor in shoulder kinematics. *Clinical Biomechanics*, 21, S3-S8. doi: 10.1016/j.clinbiomech.2005.09.007

Sides, D., & Wilson, C. (2012). Intra-limb coordinative adaptations in cycling. *Sports Biomechanics*, 11, 1-9. doi: 10.1080/14763141.2011.637118

Sinclair, J., Taylor, P.J., Edmundson, C.J., Brooks, D., & Hobbs, S.J. (2012). Influence of the helical and six available Cardan sequences on 3D ankle joint kinematic parameters. *Sports Biomechanics*, 11(3), 430-437. doi: 10.1080/14763141.2012.656762

Teu, K.K., Kim, W., Fuss, F.K., & Tan, J. (2006). The analysis of golf swing as a kinematic chain using dual Euler angle algorithm. *Journal of Biomechanics,* 39, 1227-1238. doi: 10.1016/S0021-9290(02)00241-5

van der Helm, F.C.T. (1997). A standardized protocol for motion recordings of the shoulder. *Proceedings of the First Conference of the ISG*, 7-12. Retrieved from http://internationalshouldergroup.org/files/proceedings1997/helm1.pdf

Whiteside, D., Elliott, B., Lay, B., & Reid, M. (2013). A kinematic comparison of successful and unsuccessful tennis serves across the elite development pathway. *Human Movement Science*, 32, 822-835. doi: 10.1016/j.humov.2013.06.003

Woltring, H., Huiskes, R., De Lange, A., & Veldpaus, F. (1985). Finite centroid and helical axis estimation from noisy human landmark measurements in the study of human joint kinematics. *Journal of Biomechanics*, 18, 379-389. doi: 10.1016/0021-9290(85)90293-3

Wu, G., Siegler, S., Allard, P., Kirtley, C., Leardini, A., Rosenbaum, D., ...Stokes, I. (2002). ISB recommendation on definitions of joint coordinate system of various joints for the reporting

of human joint motion – part I: ankle, hip and spine. *Journal of Biomechanics*, 35, 543-548. doi: 10.1016/S0021-9290(01)00222-6

Wu, G., van der Helm, F.C.T., Veeger, H.E.J., Makhsous, M., Van Roy, P., Anglin, C., ... Buchholz, B. (2005). ISB recommendation on definitions of joint coordinate systems of various joints for the reporting of human joint motion - Part II: shoulder, elbow, wrist and hand. *Journal of Biomechanics*, 38, 981-992. doi: 10.1016/j.jbiomech.2004.05.042

Ying, N., & Kim, W. (2002). Use of dual Euler angles to quantify the three-dimensional joint motion and its application to the ankle joint complex. *Journal of Biomechanics*, 35, 1647-57. doi: 10.1016/S0021-9290(02)00241-5

Rotation sequence to report humerothoracic kinematics during 3D motion involving large horizontal component: application to the tennis forehand drive

Table 1: Gimbal lock occurrence during the whole stroke and its three constituent phases for each of the three rotation sequences.

Rotation sequence	Whole stroke		Backswing		Forward swing		Follow-through	
	%	n	%	n	%	n	%	n
$Y_tX_f'Y_h''$	0.12 ± 0.13	4	0.09 ± 0.24	1	0.19 ± 0.27	3	**0.00 ± 0.00**	**0**
$Z_tX_f'Y_h''$	2.26 ± 4.33	3	1.66 ± 3.10	2	3.35 ± 6.78	3	**0.00 ± 0.00**	**0**
$X_tZ_f'Y_h''$	1.77 ± 1.98	7	**0.00 ± 0.00**	**0**	**0.00 ± 0.00**	**0**	9.38 ± 9.09	7

Gimbal lock occurrence was expressed both as percentages of the frames (%: mean ± standard deviation) and as the number of subjects for which at least one gimbal lock was observed among the 10 analysed trials (n). Absence of gimbal lock are marked using bold numbers.

Table 2: Averaged number of phase angle discontinuities in humerothoracic angle during the whole stroke and each of its phases for the three rotation sequences.

Rotation sequence	Rotation axis	Whole stroke	Backswing	Forward swing	Follow-through
$Y_tX_f'Y_h''$	Y_t	1.79 ± 0.61	0.38 ± 0.35	1.41 ± 0.42	**0.00 ± 0.00**
	Y_h''	1.06 ± 0.28	0.80 ± 0.33	0.03 ± 0.09	0.23 ± 0.28
$Z_tX_f'Y_h''$	Z_t	0.12 ± 0.27	0.07 ± 0.19	0.05 ± 0.09	**0.00 ± 0.00**
	Y_h''	0.12 ± 0.27	0.01 ± 0.04	0.10 ± 0.23	**0.00 ± 0.00**
$X_tZ_f'Y_h''$	X_t	0.15 ± 0.16	**0.00 ± 0.00**	**0.00 ± 0.00**	0.15 ± 0.16
	Y_h''	0.04 ± 0.08	**0.00 ± 0.00**	**0.00 ± 0.00**	0.04 ± 0.08

Bold numbers indicate the absence of phase angle discontinuities. No data were reported for the second axis as such discontinuities can occur for the first and third axes only.

Table 3: Humerothoracic angle amplitude (°) during the whole stroke and each of its phases for the three rotation sequences.

Rotation sequence	Rotation axis	Movement	Whole stroke	Backswing	Forward swing	Follow-through
$Y_tX_f'Y_h''$	Y_t	plane of elevation orientation	-0.7 ± 221.5	31.3 ± 136.7	-97.1 ± 265.3	43.2 ± 13.7
	X_f	elevation	56.0 ± 29.6	31.9 ± 25.3	-19.3 ± 31.7	43.2 ± 16.0
	Y_h	axial rotation	189.3 ± 197.9	254.9 ± 132.7	-33.7 ± 32.2	-30.1 ± 111.2
$Z_tX_f'Y_h''$	Z_t	flexion / extension	38. 7 ± 151.8	-4.3 ± 64.1	14.3 ± 62.3	**54.1 ± 21.6**
	X_f	elevation	57.5 ± 23.4	-27.0 ± 23.6	30.8 ± 16.6	**30.1 ± 13.5**
	Y_h	axial rotation	87.0 ± 126.4	-36.5 ± 22.9	-16.4 ± 108.0	**91.6 ± 26.4**
$X_tZ_f'Y_h''$	X_t	elevation	39.9 ± 91.0	**-32.0 ± 28.2**	**29.4 ± 20.2**	37.5 ± 81.6
	Z_f	flexion / extension	91.0 ± 13.3	**-6.7 ± 21.9**	**45.2 ± 16.9**	45.4 ± 11.9
	Y_h	axial rotation	-10.9 ± 101.8	**-63.2 ± 25.3**	**2.1 ± 39.0**	2.5 ± 74.4

Bold numbers indicate coherent humerothoracic angle amplitude data.

Figure 1: Definition of the Segment Coordinate Systems for the thorax (X_t, Y_t, Z_t) and humerus (X_h, Y_h, Z_h)

Figure 2: Time courses of humerothoracic joint angles obtained from $Y_tX_f'Y_h''$ (a), $Z_tX_f'Y_h''$ (b) and $X_tZ_f'Y_h''$ (c) rotation sequences during one forehand drive in one player. The discontinuities at ball-racket impact resulting from the combination of joint angles description with $X_tZ_f'Y_h''$ (before impact) and $Z_tX_f'Y_h''$ (after impact) rotation sequences are displayed in (d). Plain grey and black dashed curves correspond to axial rotation and elevation angles, respectively. Plain black curves represent plane of elevation orientation (a) and flexion / extension (b, c and d) angles. Occurrences of phase angle discontinuities (PAD) and gimbal locks (GL) are displayed in (a) and (b, c), respectively. The vertical black lines delimitate the forehand drive phases (backswing, forward swing and follow-through).

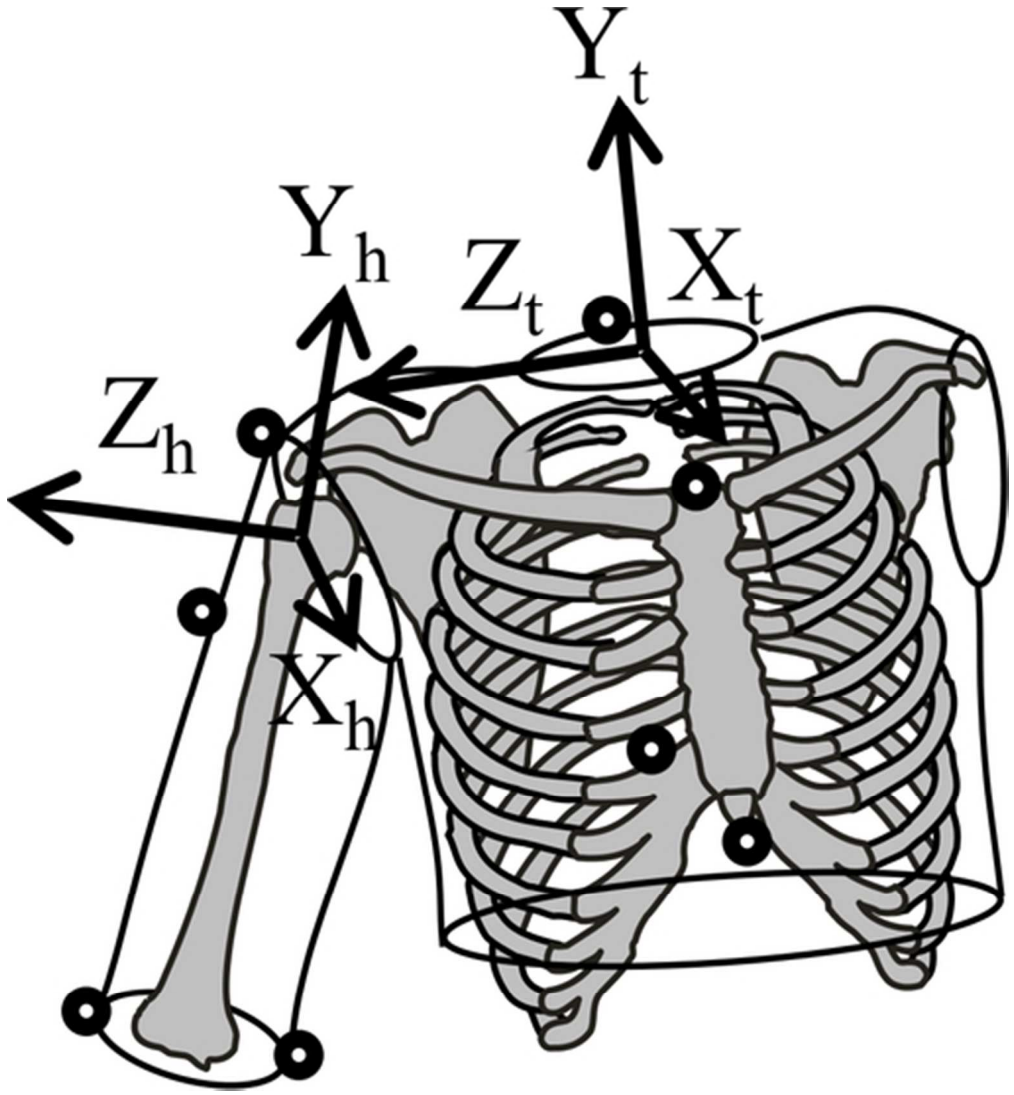

Figure 1: Definition of the Segment Coordinate Systems for the thorax (X_t, Y_t, Z_t) and humerus (X_h, Y_h, Z_h)

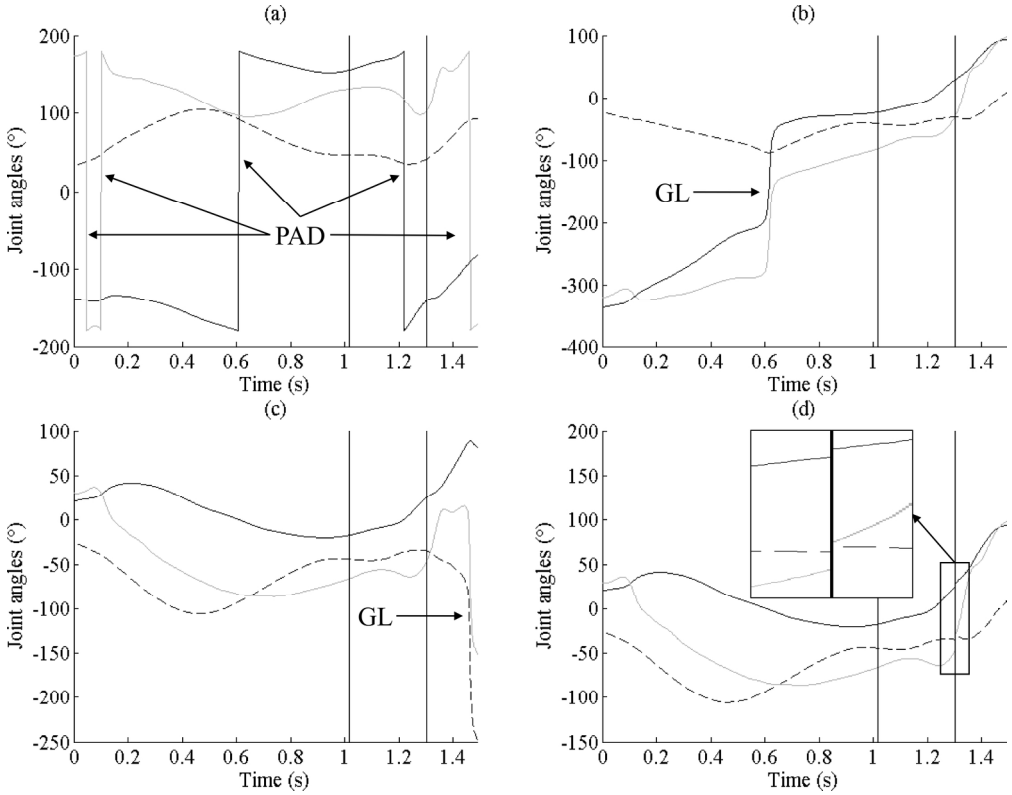

Figure 2: Time courses of humerothoracic joint angles obtained from $Y_tX_f'Y_h''$ (a), $Z_tX_f'Y_h''$ (b) and $X_tZ_f'Y_h''$ (c) rotation sequences during one forehand drive in one player. The discontinuities at ball-racket impact resulting from the combination of joint angles description with $X_tZ_f'Y_h''$ (before impact) and $Z_tX_f'Y_h''$ (after impact) rotation sequences are displayed in (d). Plain grey and black dashed curves correspond to axial rotation and elevation angles, respectively. Plain black curves represent plane of elevation orientation (a) and flexion / extension (b, c and d) angles. Occurrences of phase angle discontinuities (PAD) and gimbal locks (GL) are displayed in (a) and (b, c), respectively. The vertical black lines delimitate the forehand drive phases (backswing, forward swing and follow-through).